Nota Técnica

JUVENILE HORMONE III: SOURCE REACTIONS AND COLLISION-INDUCED DISSOCIATION IN ESI-MS/MS

Jacqueline Nakau Mendonça[a], Valquíria A. Polisel Jabor[a], Gabriel Santos Arini[a], Ricardo Roberto da Silva[a], Rafael Carvalho da Silva[b], Ricardo Vessecchi[c], Fabio Santos do Nascimento[b] and Norberto Peporine Lopes[a,*]

[a]Núcleo de Pesquisa em Produtos Naturais e Sintéticos (NPPNS), Departamento de Ciências Biomoleculares, Faculdade de Ciências Farmacêuticas de Ribeirão Preto, Universidade de São Paulo, 14040-903 Ribeirão Preto – SP, Brasil
[b]Departamento de Biologia, Faculdade de Filosofia, Ciências e Letras de Ribeirão Preto, Universidade de São Paulo, 14040-901 Ribeirão Preto – SP, Brasil
[c]Departamento de Química, Faculdade de Filosofia, Ciências e Letras de Ribeirão Preto, Universidade de São Paulo, 14040-901 Ribeirão Preto – SP, Brasil

Juvenile hormone (JH III) is an important example of a chemical signaling derived from the terpene biosynthetic pathway. Because of its impact on many species' reproductive and developmental processes, analytical approaches must be developed to accurately identify and measure it in biological samples. In this technical note, we explored the gas-phase dissociative behavior of JH III using tandem mass spectrometry combined with electrospray ionization to provide diagnostic fragment-ions for quantitative purposes.

Keywords: Juvenile hormone III; ESI, CID; gas phase chemistry; electrospray.

INTRODUCTION

All living organisms emit, detect, and respond to chemical stimuli, thus resulting in many interactions through chemical signals or cues.[1,2] In social insects, the influence of chemical signaling on the reproductive and development processes has been reported,[3,4] ranging from small hydrocarbons produced by the acetate biosynthesis pathway[5] to hormones derived from the biosynthesis of sesquiterpenes.[6] Juvenile hormone (JH III, molecular weight 266), shown in Figure 1, is an important example of a chemical signaling derived from the terpene biosynthetic pathway.[5] JH III's regulates certain stages of larval development that trigger female characteristics in bee castes.[7,8] Female larvae with high levels of JH III develop queen-like features. In stingless bees, the topical application of synthetic JH III in female larvae led to an almost total production of queens.[9] Although these examples demonstrate the value of JH III in insects, its mode of action remain unknown.[9]

In the last two decades, analytical advances in mass spectrometry in combined with -omics or focused on quantificative studies of a particular analyte have significantly expanded our understanding of the dynamics of chemical communication.[1,10] JH's analysis followed this trend, and several papers seeking to understand the dynamics of its metabolism have used high-performance liquid chromatography hyphenated to mass spectrometry.[11-17] Westerlund and Hoffman[11] and Ichikawa *et al.*[12] have monitored the sodiated adduct at *m/z* = 289; however, no fragment ion monitoring were described. Additional studies have employed a similar approach, monitoring the protonated molecule (*m/z* = 267) and the methanol elimination fragment.[13-17] Zhou *et al.*[14] have also described the neutral losses of water and methanol. Yet, none of these works describe the fragmentation mechanisms involved in forming product ions.[13] Gas-phase dissociative reactions, particularly in-source fragmentation processes, are frequently overlooked in investigations that apply ESI-MS/MS to biological samples. Knowing these processes, however, opens the possibility of discovering new metabolites or understanding biotic and abiotic stress interactions.[18] In this work, we explore the gas-phase

dissociative behavior of JH III using tandem mass spectrometry combined with electrospray ionization.

MATERIAL AND METHODS

Chemicals and reagents

HPLC grade methanol and acetonitrile were purchased from J. T. Baker (Phillipsburg, NJ, USA). The water was distilled and purified with a Millipore Milli-Q Plus System (Bedford, MA, USA). The Juvenile Hormone III, purity ≥ 65% was obtained from Sigma-Aldrich (Saint Louis, MO, USA).

LC-MS analysis

JH III solution (20 ug mL^{-1}) was directly infused into ESI-MS instruments from Waters and Bruker using methanol/water (7:3) or acetonitrile/water (7:3) and also with 0.1% formic acid. For low-resolution mass analysis, the data were acquired in a TQ detector (Waters Corp., Milford, MA, USA), and nitrogen was used as the desolvation gas (600 L h^{-1}) and as cone gas (50 L h^{-1}) at the source chamber. For collision-induced dissociation, argon was used as the collision gas. The capillary voltage was used between 1.0 to 4.0 kV for the analysis of in source reactions. Source and desolvation temperatures were 150 and 350 °C, respectively. High-resolution MS analyzes were performed on micrOTOF-QII and micrOTOF-II mass spectrometers (Bruker Daltonics, USA) with a time-of-flight analyzer (TOF). The machines were calibrated with sodium trifluoroacetic acid (TFA-Na$^+$). For MS/MS analysis in micrOTOF-QII, protonated and sodiated molecules were individually selected and fragmented at different laboratory frame collision energies, E_{lab}, (ranging from 5 to 50 eV). N$_2$ was employed as collision gas. Energy-resolved plots were obtained from ion intensities variation for each E_{lab} applied. For ESI-MS^n analysis, JH III solution (20 µg mL^{-1}) was prepared with acetonitrile/water (7:3) and acetonitrile/deuterium oxide (7:3). Analysis was carried out in an ion trap equipment (AmaZon SL, Bruker Daltonics, Massachusetts, USA) coupled with an electrospray source. Spectra were acquired in positive ionization mode (ESI$^+$),

*e-mail: npelopes@fcfrp.usp.br

with a capillary voltage of 3.5 kV. The nebulization gas used was nitrogen (N_2), with a drying temperature of 250 °C, flow rate of 5 L min^{-1}, and pressure of 15 psi. N_2 was used as the collision gas for fragmentation. Data acquisition and analysis were performed using the Bruker Compass Data Analysis 4.3 software. The MS^n parameters were: precursor 268.0; isolation width 1.0 *m/z*; fragmentation cutoff 72 *m/z*; fragmentation amplitude 1.50 V and instrument isolation with 2.7 *m/z*.

Computational methods

Protonation sites were performed using a protonation reaction between neutral and protonated species.[19,20] Computed gas-phase basicities (GB) were calculated through values for Gibbs energies from protonation reactions suggested, $M + H^+ \rightarrow MH^+$. We consider the Gibbs energies for proton as being, −6.28 kcal mol^{-1}, as described in literature.[19]

All structures had their geometries optimization and vibrational frequencies calculations at M06-2X/6-311++G(d,p)[21] level by using Gaussian 09 suite program.[22] Minima at potential energy surface were considered by analyzing of harmonic vibrational frequency in same computational level. All protonated and neutral species had only positive values of vibrational frequencies.

RESULTS AND DISCUSSION

Our initial analyzes showed that the sodium adduct was the most intense ion detected in both Waters and Bruker instruments. We also observed several dissociation products generated in the source (in-source fragments). In addition, the reactions' balance differed depending on the solvent applied or the type of source that was employed (Figure 1). Molecular ions, protonated molecules, and cationized molecules can all be formed in the ESI source (in positive mode).[23] The balance between all three ions relies on distinct processes that take place inside the capillary: the redox reaction (oxidation/reduction) that produces molecular ions, the acid/base reaction which results in the formation of protonated molecules, and the coordination with cations such as sodium or potassium.[24,25] Both the protonated and cationized "paired electron ions" tend to exhibit low internal energy, and, consequently, little or no in-source fragmentation.[26]

JH III was an exception since it generated in-source fragments even at very low capillary energies (500 V), mainly neutral elimination of methanol (Figure 2). Interestingly, no protonated molecule was observed using acetonitrile/water (7:3) as the solvent: we observed only the major sodium product and the decomposition of the protonated molecule to the ion *m/z* = 235 (loss of CH_3OH). In methanol/water, however, the in-source dissociation was less pronounced at all energies, suggesting a solvation effect providing higher stability to the protonated ion (Figure 2). The addition of formic acid (0.1% v/v) led to the complete elimination of CH_3OH,

a fact already well-detailed in the literature.[27-29] The absence of the acid in the solution, in opposition to the most common mobile phase constitution, supports the hypothesis of no interference of the capillary energy in the extension of the in-source reactions. Finally, a minor effect of in-source decomposition was observed in the quadrupole analyzer compared to TOF, suggesting that the half-life of the formed ion is short, and that methanol elimination can occur both in the capillary and during the flight.[30]

Based on these results, it would be expected to seek the development of analytical methodologies using the sodiated molecule, as with some derivatives of the acetate pathway that do not respond well to pH variations.[27,29] Therefore, we systematically analyzed the relative intensity of some product-ions of sodiated JH III *versus* laboratory collision energy (E_{lab}), displayed at supplementary material (Figure 1S). Fragment ion detection would help the development of a more robust and reliable methodology since we could work with multiple reaction monitoring modes.[31] However, the results were that no energy was applied to the formation of fragments, and only a decrease in relative intensity was observed due to the loss of coordination of sodium to JH III. These results may explain the currently uncommon use of quantifying a sodiated molecule only by the MS mode when using acid in the mobile phase is necessary.

The next step was the definition of the gas phase decomposition reactions of the protonated JH III, looking to understand the formation of major ions. Computational chemistry defined potential protonation sites for the JH III molecule. The most stable protonation site was suggested as the carbonyl group, as evidenced by the GB value, Figure 3. However, protonation at ether oxygen may occur because the differences between GB values are close 3.5 kcal mol^{-1}. Two major competitive pathways may occur for protonation and dissociation of JH III, similarly to observed for licarin A,[32] *i.e.*, where the ether oxygen atom can be the protonation site and the H_2O elimination occurred by a ring opening: (1) the methanol elimination (−32 u), through proton migration after protonation of carbonyl or (2) the water elimination (−18 u) by protonation at oxygen-like ether. In agreement with (1), when protonation takes place at the methoxyl group, dissociation is favorable with forming an acylium ion, as observed at MS/MS spectra and confirmed during the geometry's optimization using DFT calculations.

These observations can help in selecting ions for LC-MS/MS and choosing the most stable fragment ion because, as previously mentioned, the ion intensity *m/z* = 267 is compromised in the first MS, preventing the strategy of adding acid to the mobile phase. Thus, we analyze the relative intensities of product-ions *versus* collision energies for protonated JH (*m/z* = 267), shown in the supplementary material (Figure 2S). As energy increases, the signal disappears, allowing us to work with more confident ions. Our analysis (Figure 3) suggests that protonation can occur at the carbonyl group, analogous to that observed in several secondary metabolites.[32,33] This observation is consistent with the main fragmentation pathway A proposed (Figure 4), were the CH_3OH is eliminated by a charge migration
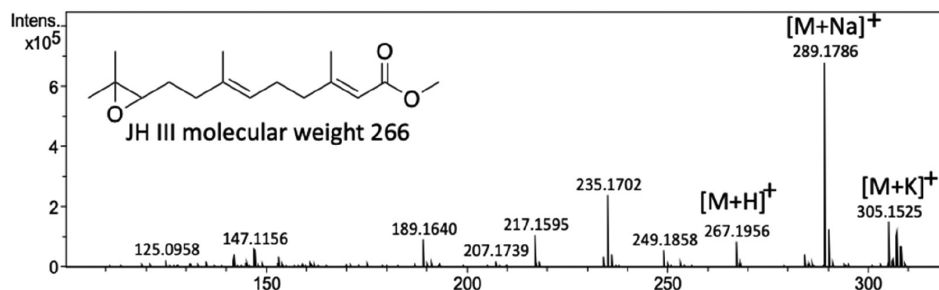
Figure 1. *Spectra of JH III showing the major ions in MS mode*
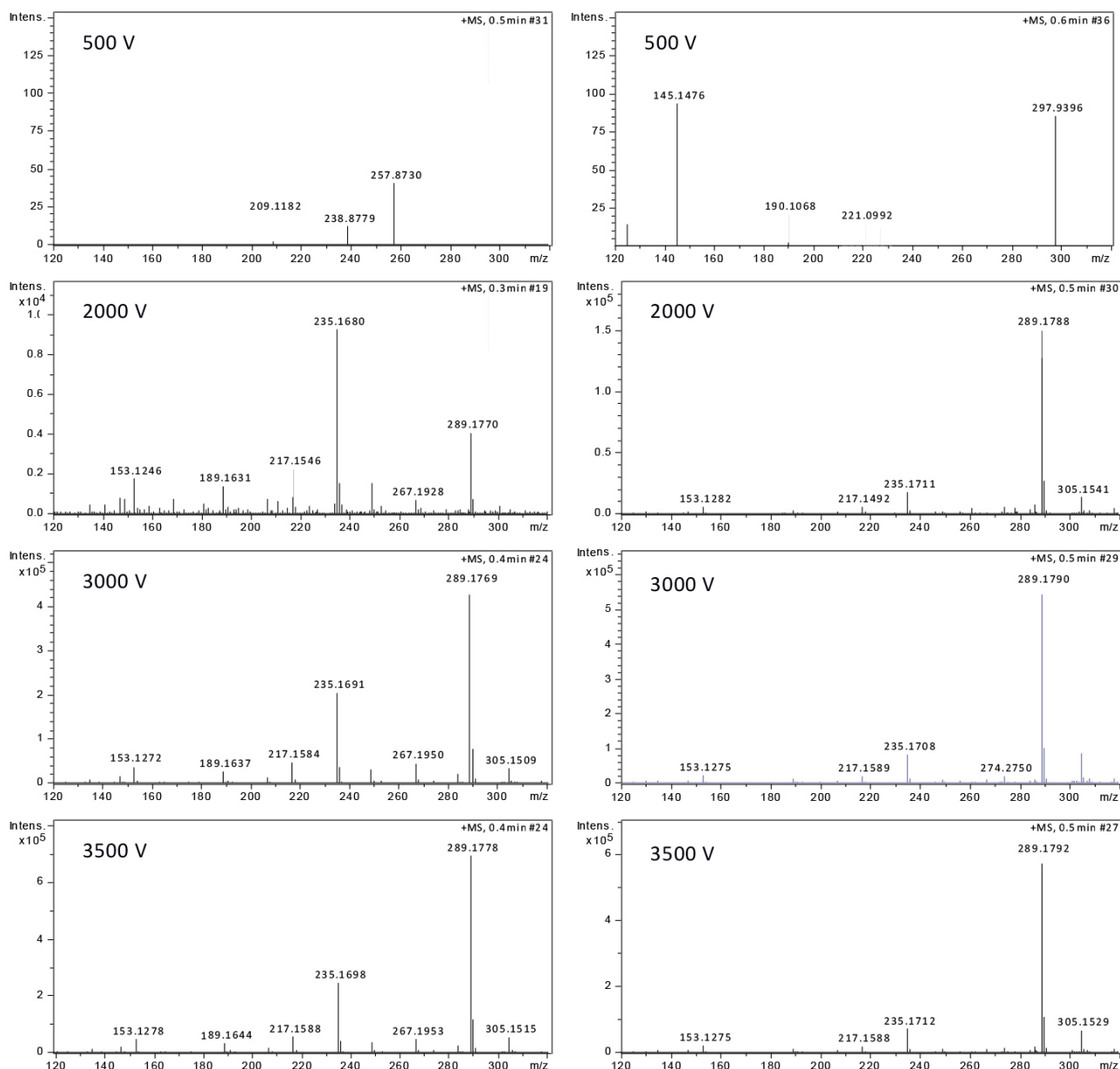
Figure 2. ESI-MS spectra of JH III in methanol/water (right column of the figure) and in acetonitrile/water (left side of the column) at different capillary energies
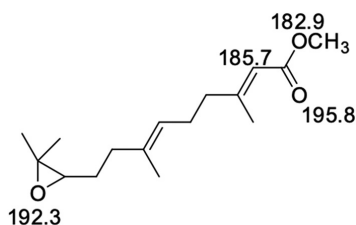
Figure 3. Gas-phase basicities, GB, calculated at level M06-2X/6-311++G(d,p)

fragmentation (CMF). Conversely, H_2O elimination could occur through CRF mechanism (Figure 3S, supplementary material), but theoretical calculations leaves margin for CMF as well (Figure 4).

To confirm the hypothesis of CMF and CRF balance, we decided to conduce MS^n experiments (at ion trap equipment) applying H_3OH/D_2O solution as solvents (20 μg mL^{-1}). Figure 4S shows an ion at m/z 268 that confirms the deuterium as the positive charge. After ion isolation and dissociation, we observed a similar fragmentation pattern (Figure 5S, supplementary material) except for dehydration,

suggesting that the neutral loss of H_2O proceeds from the opening of the epoxide substituent via CMF – with proton transfer at the ESI source – and not as described at supplementary material (Figure 3S). The theoretical calculations support the possibility of the proton binding in both positions (Figure 3), which was not observed with deuterium, demonstrating that both pathways (A and B, Figure 4) originated from CMF mechanisms.

Looking at Figure 2S (supplementary material) it is possible to observe the relative intensity of the protonated JH III, at $m/z = 267$, *versus* the ions produced via different laboratory collision energies (E_{lab}). The E_{lab} data also revealed generation of intense product-ions at m/z 153 and 135. These low molecular-weight fragments are among the three major signals at CE = 25 eV, with no significant increase of all possible precursor ions present at supplementary material (Figure 3S). Ion m/z 153 was initially proposed to be formed after methanol elimination (Figure 3S), however the MS^3 data (Figure 6S) does not confirm this pathway, suggesting its formation directly from the protonated molecule (Figure 4, pathway C). The same observation applies to the formation of ion m/z 135 (Figure 4, pathway D) since

no signal was observed in the MS³ spectrum (Figure 6S and 7S).

As part of our efforts to rationalize all mechanisms, we began with protonation at the carbonyl of the ester, implying charge migration fragmentation (CMF) reactions.[34,35] Thus, methanol elimination (pathway A) occurs as described for some esters.[32] However, CO elimination was reduced by the unsaturation in the alpha carbon of the molecule, leading to a partial stabilization of the ion $m/z = 235$. For CO elimination from $m/z = 235$, an initial isomerization of the double bond is required, as already discussed for several alkene compounds,[36] allowing spatial conformation to form a five-member ring and one tertiary carbocation, as proposed in Figure 4 (pathway A, ion at $m/z = 207$). However, collision energies need to be lower than 25 eV to allow for this ion to occur and its successive dehydration. On the other hand, at higher CEs, $m/z = 235$ forms a very intense ion with the potential to be monitored in quantitative studies. This product-ion derived from neutral elimination of water from the epoxide group. In this case, a ring-opening reaction is required, followed by H_2O elimination by a remote hydrogen rearrangement[35] forming the ion at $m/z = 217$. The next reaction was again remote hydrogen rearrangement[35] losing an alkene at ($m/z = 175$) and this

ion structure can isomerize, as already explained, and eliminate CO, forming the ion at $m/z = 149$. Ion trap analysis (see supplementary material, Figure 6S) confirms that these ions come from pathway A.

In addition to the pathway A, we observed the formation of ion m/z 249 (Figure 4). This ion can undergo a CMF reaction to generate the ion at $m/z = 217$ with proton retention. MS³ experiment shows an alternative fragmentation route (pathway B) with one additional fragment (at $m/z = 189$), also formed after isomerization (Figure 4). At CEs between 25 to 35 eV, $m/z = 135$ becomes the main fragment, and its formation is derived from heterolytic cleavage of the carbon-carbon bond assisted by the positive charge of the conjugated protonated carboxylic acid moiety (Figure 4, pathway C). The resulting fragment is an allylic carbocation with good stability, which can explain the ion intensity in Figure 2S (supplementary material) and its absence in MS³ spectra of the fragment m/z at 235. The last pathway D (Figure 4) can be explained by a concerted mechanism driven by the charge at the epoxy group.

Generally, protonated molecules dissociate by charge retention fragmentation type (CRF) mechanisms; in these cases, no carbocations are formed, and instead, we see neutral eliminations
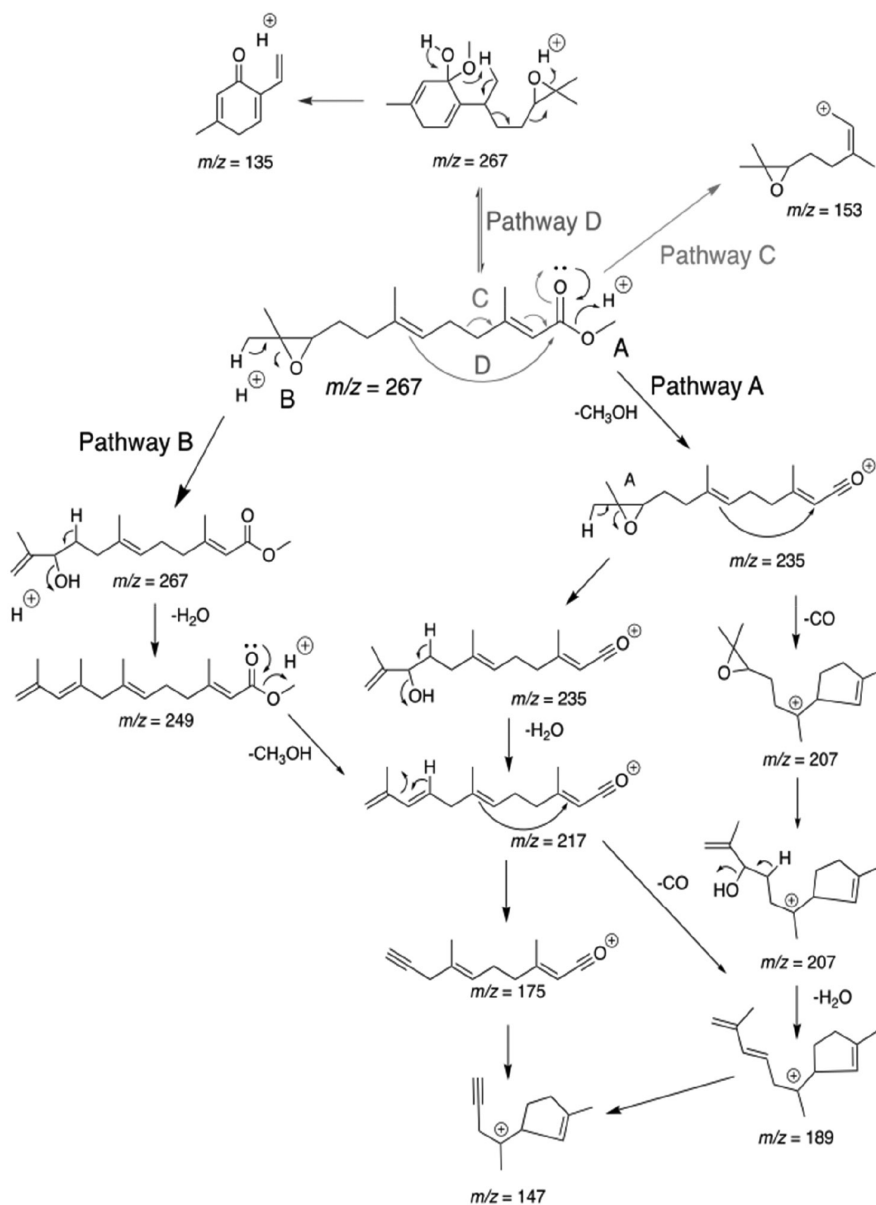
Figure 4. *Proposed fragmentation pathway of protonated ion of JH III*

regardless of the charge transferred to the molecule's most basic site.[35] The physicochemical properties of JH III, however, suggested that most fragment-ions originated from a CMF-type fragmentation process, uncommon in ESI-MS/MS spectra. These findings were supported by computational calculation and contributed to the first description of a rational fragmentation mapping of the protonated JH III molecule in ESI-MS/MS and ESI-MS^n.

CONCLUSION

The study presented in this technical note provides valuable insights into the gas-phase dissociative behavior of Juvenile hormone III (JH III) using tandem mass spectrometry combined with electrospray ionization. While previous research has focused on analyzing JH III through high-performance liquid chromatography hyphenated to mass spectrometry, this study delves into the chemistry of JH III in the gaseous phase, explicitly examining the decomposition of selected ions in the collision chamber. The results demonstrate that JH III exhibits unique in-source fragmentation patterns, generating various dissociation products even at low capillary energies. Furthermore, the choice of solvent and type of mass spectrometer employed also influence the reactions' balance and the formation of different ions. Notably, the fragmentation mechanisms involved in forming product ions are described, shedding light on potential metabolites and stress interactions. Overall, this comprehensive analysis lays the groundwork for future quantitative studies of JH III using mass spectrometry techniques and highlights the importance of considering gas-phase dissociation processes in biological sample analysis.

SUPPLEMENTARY MATERIAL

Complementary material for this work is available at http://quimicanova.sbq.org.br/, as a PDF file, with free access.

ACKNOWLEDGMENTS

REFERENCES

1. Brunetti, A. E.; Carnevale Neto, F.; Vera, M. C.; Taboada, C.; Pavarini, D. P.; Bauermeister, A.; Lopes, N. P.; *Chem. Soc. Rev.* **2018**, *47*, 1574. [Crossref]

2. Nunes T. M.; Turatti, I. C. C.; Mateus, S.; Nascimento, F. S.; Lopes, N. P.; Zucchi, R.; *GMR, Genet. Mol. Res.* **2009**, *8*, 589. [Link] accessed in August 2023

3. Nunes, T. M.; Mateus, S.; Favaris, A. P.; Amaral, M. F. Z. J.; von Zuben, L. G.; Clososki, G. C.; Bento, J. M. S.; Oldroyd, B. P.; Silva, R.; Zucchi, R.; Silva, D. B.; Lopes, N. P.; *Sci. Rep.* **2014**, *4*, 7449. [Crossref]

4. Wyatt, G. R.; Davey K. G.; *Adv. Insect Physiol.* **1996**, *26*, 1. [Crossref]

5. Nunes, T. M.; Oldroyd, B. P.; Elias, L. G.; Mateus, S.; Turatti, I. C.; Lopes, N. P.; *Nature Ecology & Evolution* **2017**, *1*, 185. [Crossref]

6. Shinoda, T. In *Handbook of Hormones*; Takei, Y., Ando, H., Tsutsui, K., eds.; Academic Press: New York, 2016, ch. 99. [Crossref]

7. Asencot, M.; Lensky, Y.; *Insect Biochem.* **1988**, *18*, 127. [Crossref]

8. Hartfelder, K.; Makert, G. R.; Judice, C. C.; Pereira, G. A. G.; Santana, W. C.; Dallacqua, R.; Bitondi, M. M. G.; *Apidologie* **2006**, *37*, 144. [Crossref]

9. Campos, L. A. O.; Velthuis, H. H. W.; Velthuis-Kluppell, F. M.; *Die Naturwissenchaften* **1975**, *62*, 98. [Link] accessed in August 2023

10. Demarque, D. P.; Dusi, R. G.; de Sousa, F. D. M.; Grossi, S. M.; Silvério, M. R. S.; Lopes, N. P.; Espindola, L. S.; *Sci. Rep.* **2020**, *10*, 1051. [Crossref]

11. Westerlund, S. A.; Hoffmann, K. H.; *Anal. Bioanal. Chem.* **2004**, *379*, 540. [Crossref]

12. Ichikawa, A.; Ono, H.; Furuta, K.; Shiotsuki, T.; Shinoda, T.; *J. Chromatogr. A* **2007**, *1161*, 252. [Crossref]

13. Chen, Z.; Linse, K. D.; Taub-Montemayor, T. E.; Rankin, M. A.; *Insect Biochem. Mol. Biol.* **2007**, *37*, 799. [Crossref]

14. Zhou, J.; Qi, Y.; Hou, Y.; Zhao, J.; Li, Y.; Xue, X.; Wu, L.; Zhang, J.; Chen, F.; *J. Chromatogr. B: Anal. Technol. Biomed. Life Sci.* **2011**, *879*, 2533. [Crossref]

15. Ares, A. M.; Nozal, M. J.; Bernal, J. L.; Martín-Hernàndez, R.; Higes, M.; Bernal, J.; *J. Chromatogr. B: Anal. Technol. Biomed. Life Sci.* **2012**, *899*, 146. [Crossref]

16. Ramirez, C. E.; Nouzova, M.; Benigni, P.; Quirke, M.; Noriega, F. G.; *Talanta* **2016**, *159*, 371. [Crossref]

17. Ramirez, C. E.; Nouzova, M.; Michalkova, V.; Fernandez-Lima, F.; Noriega, F. G.; *Insect Biochem. Mol. Biol.* **2020**, *116*, 103287. [Crossref]

18. Bueno, P. C. P.; Lopes, N. P.; *ACS Omega* **2020**, *5*, 1752. [Crossref]

19. Range, K.; Riccardi, D.; Cui, Q.; Elstner, M.; York, D. M.; *Phys. Chem. Chem. Phys.* **2005**, *7*, 3070. [Crossref]

20. Deakyne, C. A.; *Int. J. Mass Spectrom.* **2003**, *227*, 601. [Crossref]

21. Zhao, Y.; Truhlar, D. G.; *J. Phys. Chem. A* **2008**, *112*, 1095. [Crossref]

22. Frisch, M. J.; Trucks, G. W.; Schlegel, H. B.; Scuseria, G. E.; *Gaussian 09, Revision D.01*, Gaussian, Inc., Wallingford CT, 2009.

23. Crotti, A. E. M.; Vessecchi, R.; Lopes, J. L. C.; Lopes, N. P.; *Quim. Nova* **2006**, *29*, 287. [Crossref]

24. Guaratini, T.; Vessecchi, R. L.; Lavarda, F. C.; Campos, P. M. B. G. M.; Naal, Z.; Gates, P. J.; Lopes, N. P.; *Analyst* **2004**, *129*, 1223. [Crossref]

25. Guaratini, T.; Vessecchi, R.; Pinto, E.; Collepicolo, P.; Lopes, N. P.; *J. Mass Spectrom.* **2005**, *40*, 963. [Crossref]

26. Fenn, J. B.; Mann, M.; Meng, C. K.; Wong, S. F.; Whitehouse, C. M.; *Science* **1989**, *246*, 64. [Crossref]

27. Lopes, N. P.; Stark, C. B. W.; Hong, H.; Gates, P. J.; Staunton, J.; *Analyst* **2001**, *126*, 1630. [Crossref]

28. Liigand, J.; Laaniste, A.; Kruve, A.; *J. Am. Soc. Mass Spectrom.* **2017**, *28*, 461. [Crossref]

29. Lopes, N. P.; Stark, C. B. W.; Gates, P. J.; Staunton, J.; *Analyst* **2002**, *127*, 503. [Crossref]

30. Dias, H. J.; Melo, N. I.; Crotti, A. E. M. In *Tandem Mass Spectrometry - Applications and Principles*; Prasain, J. K., ed.; IntechOpen: London, 2012, ch. 25. [Crossref]

31. Fu, Q.; Chen, Z.; Zhang, S.; Parker, S. J.; Fu, Z.; Tin, A.; Liu, X.; Van Eyk, J. E. In *Quantitative Proteomics by Mass Spectrometry*; Sechi, S., ed.; Humana Press: New York, 2016, p. 294. [Crossref]

32. Souza, J. N. P. E.; da Silva, R. M.; Fortes, S. S.; de Oliveira, A. R. M.; Ferreira, L. S.; Vessecchi, R.; Lopes, N. P.; Silva, D. B.; *Planta Med.* **2023**, *89*, 700. [Crossref]

33. Crotti A. E. M.; Lopes, J. L. C.; Lopes, N. P.; *J. Mass Spectrom.* **2005**, *40*, 1030. [Crossref]

34. Martínez-Cifuentes, M.; Clavijo-Allancan, G.; Zuñiga-Hormazabal, P.; Aranda, B.; Barriga, A.; Weiss-López, B.; Araya-Maturana, R.; *Int. J. Mol. Sci.* **2016**, *17*, 1071. [Crossref]

35. Demarque, D. P.; Crotti, A. E. M.; Vessecchi, R.; Lopes, J. L. C.; Lopes, N. P.; *Nat. Prod. Rep.* **2016**, *33*, 432. [Crossref]

36. Guaratini, T.; Lopes, N. P.; Pinto, E.; Collepicolo, P.; Gates, P. J.; *Chem. Commun.* **2006**, *39*, 4110. [Crossref]